

Hexaruthenium carbido carbonyl methyl cluster $[\text{PPN}][\text{Ru}_6\text{C}(\text{CO})_{16}(\text{CH}_3)]$ as catalyst precursor for hydrogenation of olefins. Syntheses and structures of unsaturated and saturated hexaruthenium hydrido clusters $[\text{PPN}][\text{Ru}_6\text{C}(\text{CO})_{15}\text{H}]$ and $[\text{PPN}][\text{Ru}_6\text{C}(\text{CO})_{16}\text{H}]$

T. Chihara and H. Yamazaki¹

The Institute of Physical and Chemical Research (RIKEN), Wako-shi, Saitama 351-01 (Japan)

(Received January 12, 1994; in revised form February 23, 1994)

Abstract

Cluster $[\text{PPN}][\text{Ru}_6\text{C}(\text{CO})_{16}(\text{CH}_3)]$ (**2**) has been found to be catalytic active for the hydrogenation and isomerization of olefins at 60°C after an induction period. Reaction of **2** or $[\text{PPN}][\text{Ru}_6\text{C}(\text{CO})_{15}(\text{C}_3\text{H}_5)]$ with dihydrogen at 130°C gives an unsaturated hydrido cluster $[\text{PPN}][\text{Ru}_6\text{C}(\text{CO})_{15}\text{H}]$ (**6**), which behaves as the catalyst at ambient temperature. The structure of **6** has a carbon-centered octahedral geometry of ruthenium atoms which is surrounded by fifteen carbonyl ligands, two terminal ones for each ruthenium atom and three bridging ones, and a bridging hydrido ligand. Treatment of **6** with carbon monoxide yields a saturated hydrido cluster $[\text{PPN}][\text{Ru}_6\text{C}(\text{CO})_{16}\text{H}]$ (**5**), which is also prepared by protonation of $[\text{PPN}]_2[\text{Ru}_6\text{C}(\text{CO})_{16}]$. X-ray analysis of **5** shows the cluster anion is disordered between two sites in the ratio of 8 to 2. The major one contains a carbon centered octahedron of six ruthenium atoms with two terminal carbonyl ligands for each ruthenium atom, with four bridging carbonyl ligands, and a terminal hydrido ligand.

Key words: Ruthenium; Carbide; Carbonyl; Cluster; Catalyst precursor

1. Introduction

Metal cluster compounds have drawn much attention as possible new source of homogeneous catalyst, because polynuclear coordination could induce reactivity into a ligand that differs significantly from that produced by mononuclear coordination, and the presence of adjacent metals could help to promote multiple addition of reactants and electrons to a ligand. However, there are few reports on homogeneous catalysis that are characteristic of metal cluster [1]. This may be ascribed to the cluster skeleton readily breaking down under reaction conditions. We have been interested in the use of clusters having an encapsulated element in the cavity of the metal polyhedra [2] as catalyst, be-

cause the interstitial element is expected to support inherently-weak metal–metal bonds, from the inside of the metal skeleton without disturbing the coordination of reactants on the “cluster surface.” We selected the dianionic ruthenium cluster $[\text{PPN}]_2[\text{Ru}_6\text{C}(\text{CO})_{16}]$ (**1**) [3] as starting material and succeeded to prepare its methyl, $[\text{PPN}][\text{Ru}_6\text{C}(\text{CO})_{16}(\text{CH}_3)]$ (**2**), acetyl, $[\text{PPN}][\text{Ru}_6\text{C}(\text{CO})_{16}(\text{COCH}_3)]$, and allyl, $[\text{PPN}][\text{Ru}_6\text{C}(\text{CO})_{15}(\mu\text{-}\eta^3\text{-C}_3\text{H}_5)]$ (**3**), derivatives without breaking down of the metal framework of the parent compound [4]. Here we describe the use of **2** as a successful catalyst precursor for the hydrogenation and isomerization of olefins, and isolation of the resulting catalytically-active coordinatively-unsaturated hydrido cluster.

Previously we reported the preparation of the hydrido cluster $[\text{PPh}_4][\text{Ru}_6\text{C}(\text{CO})_{16}\text{H}]$ (**4**) by protonation of the corresponding dianion $[\text{PPN}]_2[\text{Ru}_6\text{C}(\text{CO})_{16}]$ [5]. We also report here the preparation of **4** and $[\text{PPN}][\text{Ru}_6\text{C}(\text{CO})_{16}\text{H}]$ (**5**) by a different route, addition of

Correspondence to: Dr. T. Chihara.

¹ Present address: Department of Applied Chemistry, Chuo University, Kasuga, Bunkyo-ku, Tokyo 112, Japan.

carbon monoxide to the unsaturated cluster, and the X-ray analysis of **5**, which revealed a different structure of the anionic moiety.

2. Results and discussion

2.1. Hydrogenation of olefin with $[PPN][Ru_6C(CO)_{16}(CH_3)]$ (**2**) as catalyst precursor

In the presence of a catalytic amount of cluster **2** hydrogenation of 3-methyl-1-butene (**3m1b**) could not be observed at room temperature and under 100 atm of dihydrogen. However, at 60°C the hydrogenation reaction took place after an induction period of *ca.* 2 h. When **2** was kept at 80°C for 2 h under 100 atm of dihydrogen prior to introducing **3m1b**, the hydrogenation took place even at room temperature without any induction period. The reaction profile of **3m1b** is represented in Fig. 1. The isomerization of **3m1b** into 2-methyl-2-butene (**2m2b**) and 2-methyl-1-butene (**2m1b**) occurred to an appreciable extent concurrently with the hydrogenation into 2-methylbutane (**2mb**). By comparison **3m1b** was hydrogenated on charcoal-supported ruthenium metal (Ru-charcoal), and the reaction profile, shown in Fig. 2, indicates that hydrogenation was predominant. Similarly, the hydrogenation of **2m2b** or **2m1b** by **2** proceeded concurrently with isomerization in appreciable extent, but the hydrogenation by Ru-charcoal proceeded to give only the hydrogenation product **2mb**. The rates of hydrogenation of **3m1b** were measured in the temperature range of 20 to 80°C using **2** and Ru-charcoal, and the activation ener-

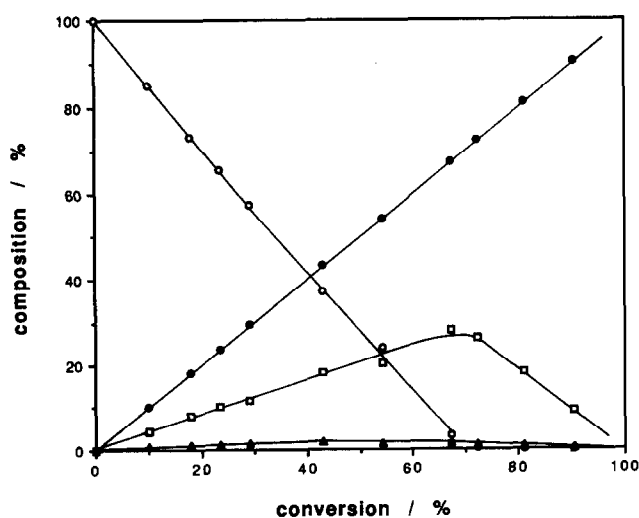


Fig. 1. The hydrogenation profile of 3-methyl-1-butene (**3m1b**) by pretreated $[PPN][Ru_6C(CO)_{16}(CH_3)]$ (**2**) with dihydrogen as the catalyst; at 60°C under 100 atm of dihydrogen in THF, 3-methyl-1-butene (**3m1b**) (○), 2-methyl-2-butene (**2m2b**) (□), 2-methyl-1-butene (**2m1b**) (△), and 2-methylbutane (**2mb**) (●).

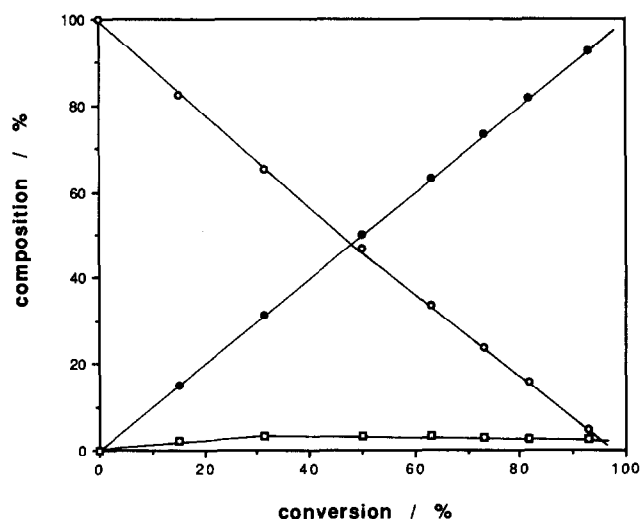


Fig. 2. The hydrogenation profile of 3-methyl-1-butene (**3m1b**) by Ru-charcoal; at 60°C under 100 atm of dihydrogen in THF, 3-methyl-1-butene (**3m1b**) (○), 2-methyl-2-butene (**2m2b**) (□), and 2-methylbutane (**2mb**) (●).

gies were calculated as 11.7 ± 0.3 and 8.5 ± 0.6 Kcal mol⁻¹, respectively.

Cyclohexanone and benzene were hydrogenated by both catalysts. However, **2** was found to be inactive for the hydrogenation of nitrobenzene to aniline, in contrast to Ru-charcoal. It is well known that the hydrogenation of nitrobenzene proceeds very readily when using Group VIII metal catalysts [6].

When isoprene was hydrogenated by **2**, the selectivity of the half-hydrogenated products (**2m1b**, **2m2b**, and **3m1b**) is 67% at the initial stage of the reaction, which is in contrast with the 38% for Ru-charcoal yielding the completely-hydrogenated product (**2mb**) as the main product.

These results suggest that the active species in these hydrogenations is not the bulk metal [7] produced by the decomposition of **2**, but a cluster species produced from **2**.

2.2. Reaction profile of $[PPN][Ru_6C(CO)_{16}(CH_3)]$ (**2**) and $[PPN][Ru_6C(CO)_{15}(C_3H_5)]$ (**3**) with dihydrogen

Treatment of **2** in methanol with 1 atm of dihydrogen at 100°C for 1 h in a Pyrex ampoule produced methane in 85% yield, suggesting the formation of a hydrido cluster.

Reaction of **3** with dihydrogen is represented in Figs. 3 and 4. As shown in Fig. 3, the reaction at 110°C for 1 h gave mainly propylene and a little amount of propane, though the combined yield was as low as 4%. This figure also shows that the combined yield increases up to 99%, but the relative content of propylene decreases upon prolonged reaction times. These

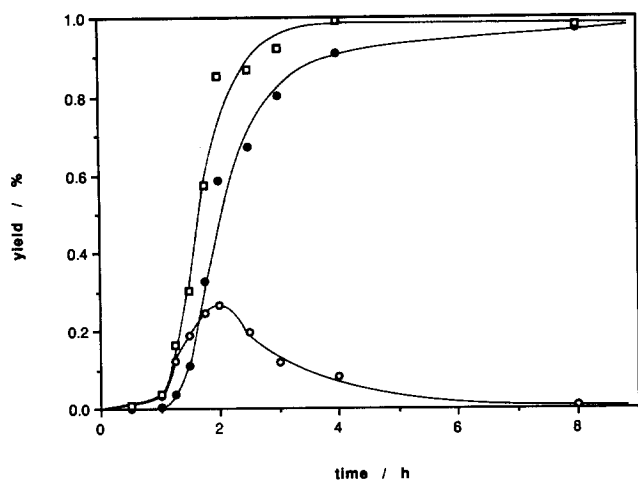


Fig. 3. The effect of time on the reaction of $[PPN][Ru_6C(CO)_{15}-(C_3H_5)]$ (**3**) with dihydrogen at 110°C in methanol under 1 atm of dihydrogen; propylene (\circ), propane (\bullet), and the combined amount of them (\square).

findings indicate that the propylene is released first from cluster **3** and then hydrogenated into propane by the catalytically-active species produced from **3**.

As shown in Fig. 4, the reaction profile obtained by changing the reaction temperature is somewhat different from that obtained at constant temperature (Fig. 3). Up to 130°C the two reaction profiles are similar, but at temperatures over 160°C the propylene produced was left intact. The inside of the glass ampoules for these experiments became coated with a metal mirror produced by decomposition of the cluster, and the red solution of **3** turned clear. No such metal mirror was observed in the experiments made at temperatures below 130°C. These results clearly indicate

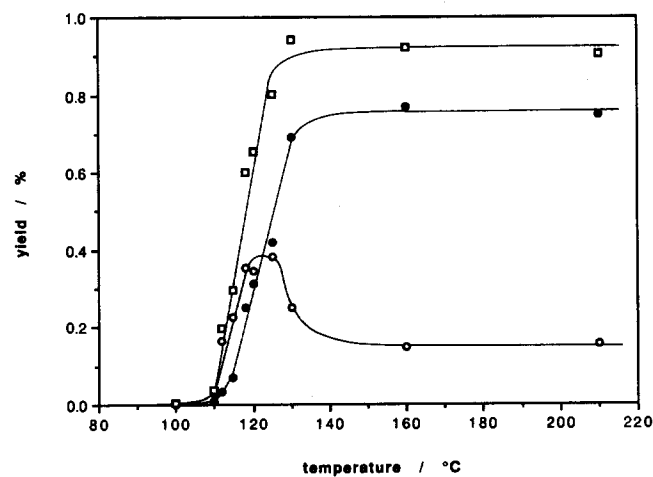


Fig. 4. The effect of temperature on the reaction of $[PPN][Ru_6C(CO)_{15}(C_3H_5)]$ (**3**) with 1 atm of dihydrogen for 1 h in methanol; propylene (\circ), propane (\bullet), and the combined amount of them (\square).

that the bulk metal produced by decomposition of the metal cluster has no significant activity in the catalytic hydrogenation of propylene.

2.3. Synthesis and structure of $[PPN][Ru_6C(CO)_{15}H]$ (**6**)

In attempt to isolate the catalytically-active species, **2** was treated in methanol with dihydrogen (100 atm) at 100°C for 1 h in an autoclave. Work-up of the reaction mixture afforded red crystals in a good yield. The IR spectrum was similar to that of **2** showing a strong absorption band at 2009 cm^{-1} in the $\nu(C=O)$ region. This indicates that the product is mono-anionic, because the frequency is an intermediate of those of the dianion $[Et_4N]_2[Ru_6C(CO)_{16}]$ (1978 cm^{-1}) [**3**] and the neutral complex $Ru_6C(CO)_{17}$ (2064 cm^{-1}) [**8**]. The 1H NMR spectrum of the product showed a complex multiplet at δ 7.4–7.9 owing to phenyl protons of the $[PPN]$ cation and a singlet at -20.01 attributable to a hydrido whose peak areas are in a ratio of 30:1. There is no indication of any other signals in the region of δ -100 to 100. On the basis of these spectroscopic data, and the elemental analyses, the resulting complex was assumed to be a mono-anionic carbido hydrido carbonyl hexanuclear ruthenium cluster. The same product was obtained by treatment of **3** with dihydrogen.

In order to obtain the exact molecular structure of the hydrido cluster a single-crystal X-ray diffraction study was undertaken. The cluster was proved to be $[PPN][Ru_6C(CO)_{15}H]$ (**6**), and the structure of the anionic part is shown in Fig. 5. The selected interatomic distances and bond angles are listed in Tables 1 and 2, respectively.

The octahedral metal skeleton of **2** remains in **6**. The metal–metal distances in **6** range from 2.8620(8) to 2.9558(8) Å, and the carbonyl bridged Ru(2)–Ru(3) edge is the shortest metal–metal bond in this cluster. The second and third shortest metal–metal bonds are the carbonyl semi-bridged edges Ru(4)–Ru(5) and Ru(5)–Ru(6). The average unbridged metal–metal distance is 2.900(9) Å, which essentially is equal to that in **2** (2.903(14) Å). Thus, the metal–carbide bond lengths in **6** (mean 2.051(9) Å) are similar to those in **2** (mean 2.054(13) Å).

There are fifteen carbonyl ligands in **6**. One carbonyl ligand, C(23)O(23), bridges the Ru(2)–Ru(3) edge, with metal–carbon bond lengths 2.120(7) Å to Ru(2) and 2.036(7) Å to Ru(3). Two carbonyl ligands, C(45)O(45) and C(56)O(56), asymmetrically bridge the Ru(4)–Ru(5) and Ru(5)–Ru(6) edges, respectively. In both cases the longer metal–carbon bond lengths are to Ru(5) (Ru(4)–C(45), 1.985(8); Ru(5)–C(45), 2.301(9); Ru(5)–C(56), 2.299(8); Ru(6)–C(56) 2.017(7) Å). The remaining twelve carbonyl ligands, two for each ruthenium

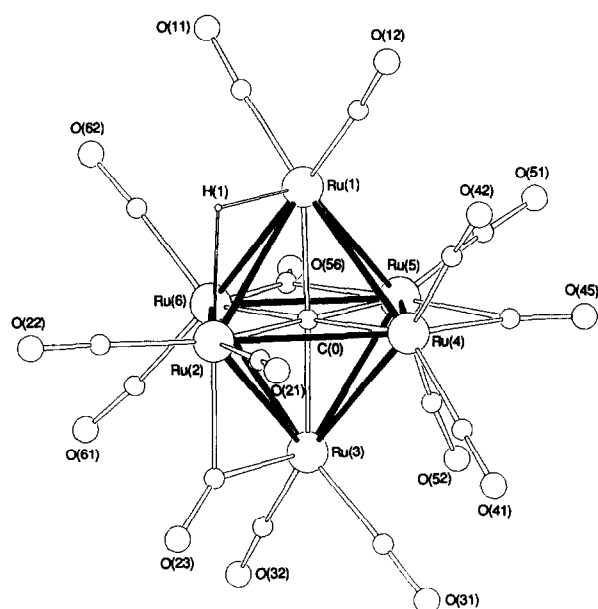


Fig. 5. The molecular structure of $[\text{Ru}_6\text{C}(\text{CO})_{15}\text{H}]^-$ (anion of **6**), with the numbering of the oxygen atoms corresponding to that of the relevant carbonyl carbon atoms. The first digit of each oxygen number is the number of the ruthenium atom to which the carbonyl is attached.

nium atom, are terminal with Ru–C bond distances 1.864(9)–1.920(8) Å (average 1.891(5) Å), C–O distances 1.110(10)–1.154(10) Å (average 1.138(4) Å), and Ru–C–O angles 169.5(8)–178.7(9)° (average 175.8(8)°). The C–O distances are shorter than those for the bridging carbonyls.

One hydrogen atom (H(1)) in the cluster was revealed by difference Fourier syntheses. This bridges

TABLE 1. Selected interatomic distances (Å) and esd values for $[\text{PPN}][\text{Ru}_6\text{C}(\text{CO})_{15}\text{H}]$ (**6**)

Ru(1)–Ru(2)	2.9133(8)	Ru(4)–C(0)	2.018(7)
Ru(1)–Ru(4)	2.8903(9)	Ru(5)–C(0)	2.076(7)
Ru(1)–Ru(5)	2.9141(9)	Ru(6)–C(0)	2.053(7)
Ru(1)–Ru(6)	2.8731(7)	Ru(1)–H(1)	1.79(8)
Ru(2)–Ru(3)	2.8620(8)	Ru(2)–H(1)	2.02(8)
Ru(2)–Ru(4)	2.9558(8)	Ru(2)–C(23)	2.120(7)
Ru(2)–Ru(6)	2.9223(8)	Ru(3)–C(23)	2.036(7)
Ru(3)–Ru(4)	2.8901(8)	Ru(4)–C(45)	1.985(8)
Ru(3)–Ru(5)	2.9551(8)	Ru(5)–C(45)	2.310(9)
Ru(3)–Ru(6)	2.8865(9)	Ru(5)–C(56)	2.299(8)
Ru(4)–Ru(5)	2.8698(8)	Ru(6)–C(56)	2.017(7)
Ru(5)–Ru(6)	2.8706(9)	O(23)–C(23)	1.170(9)
Ru(1)–C(0)	2.040(7)	O(45)–C(45)	1.144(11)
Ru(2)–C(0)	2.070(7)	O(56)–C(56)	1.162(9)
Ru(3)–C(0)	2.049(7)		

TABLE 2. Selected interatomic angles (°) and esd values for $[\text{PPN}][\text{Ru}_6\text{C}(\text{CO})_{15}\text{H}]$ (**6**)

C(0)–Ru(1)–C(11)	137.8(3)	C(41)–Ru(4)–C(45)	93.0(4)
C(0)–Ru(1)–C(12)	135.0(3)	C(42)–Ru(4)–C(45)	97.0(3)
C(0)–Ru(1)–H(1)	89(2)	C(0)–Ru(5)–C(45)	88.1(3)
C(11)–Ru(1)–C(12)	87.1(4)	C(0)–Ru(5)–C(51)	157.2(3)
C(11)–Ru(1)–H(1)	90(3)	C(0)–Ru(5)–C(52)	112.1(3)
C(12)–Ru(1)–H(1)	90(2)	C(0)–Ru(5)–C(56)	89.8(3)
C(0)–Ru(2)–C(21)	114.3(3)	C(45)–Ru(5)–C(51)	88.6(3)
C(0)–Ru(2)–C(22)	156.1(4)	C(45)–Ru(5)–C(52)	90.9(4)
C(0)–Ru(2)–C(23)	91.0(3)	C(45)–Ru(5)–C(56)	177.1(3)
C(0)–Ru(2)–H(1)	82.(2)	C(51)–Ru(5)–C(52)	90.5(4)
C(21)–Ru(2)–C(22)	89.1(4)	C(51)–Ru(5)–C(56)	94.2(3)
C(21)–Ru(2)–C(23)	91.6(3)	C(52)–Ru(5)–C(56)	88.1(4)
C(21)–Ru(2)–H(1)	95(2)	C(0)–Ru(6)–C(61)	98.9(3)
C(22)–Ru(2)–C(23)	93.3(3)	C(0)–Ru(6)–C(62)	133.3(3)
C(22)–Ru(2)–H(1)	92(2)	C(56)–Ru(6)–C(61)	93.6(3)
C(23)–Ru(2)–H(1)	172(2)	C(56)–Ru(6)–C(62)	90.9(3)
C(0)–Ru(3)–C(23)	94.0(3)	C(61)–Ru(6)–C(62)	90.9(4)
C(0)–Ru(3)–C(31)	133.0(3)	Ru(2)–C(23)–Ru(3)	87.0(3)
C(0)–Ru(3)–C(32)	136.1(3)	Ru(2)–C(23)–O(23)	134.7(6)
C(23)–Ru(3)–C(31)	94.5(4)	Ru(3)–C(23)–O(23)	138.3(6)
C(23)–Ru(3)–C(32)	96.9(3)	Ru(4)–C(45)–Ru(5)	83.5(3)
C(31)–Ru(3)–C(32)	88.4(4)	Ru(4)–C(45)–O(45)	147.7(7)
C(0)–Ru(4)–C(41)	135.3(3)	Ru(5)–C(45)–O(45)	128.8(7)
C(0)–Ru(4)–C(42)	131.7(3)	C(0)–Ru(4)–C(45)	99.4(3)
C(0)–Ru(4)–C(45)	99.4(3)	Ru(5)–C(56)–Ru(6)	83.1(3)
C(41)–Ru(4)–C(42)	88.4(4)	Ru(5)–C(56)–O(56)	129.0(6)
Ru(6)–C(56)–O(56)	148.0(7)	Ru(1)–H(1)–Ru(2)	99(4)

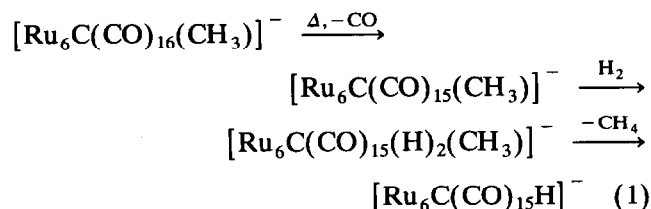
the Ru(1)–Ru(2) edge, with the shorter metal–hydrido interaction (1.79(8) Å) to Ru(1) and the longer metal–hydrido interaction (2.02(8) Å) to Ru(2).

The ligand distribution in **6** is similar to that in $[\text{Ph}_4\text{As}]_2[\text{Ru}_6\text{C}(\text{CO})_{16}]$ [9], whose anion consists of two terminal carbonyl ligands per ruthenium atom and four edge-bridging carbonyl ligands, giving an approximate overall D_{2d} symmetry. Replacement of one of the bridging carbonyl in the anion by a bridging hydrido gives the anion of **6** with C_s symmetry. In each case, a set of bridging ligands interacts with a common ruthenium atom having the longer metal–carbon or metal–hydrogen bond lengths.

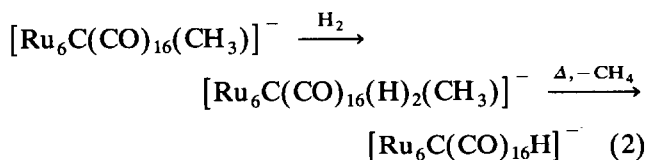
The anionic cluster of **6** has 84 valence electrons, which is 2 less than the 86 valence electrons predicted by the PSEP approach, for the hexanuclear octahedral clusters such as **1**, **2**, and **3** [10]. Localization of the unsaturation on a special Ru–Ru edge could not be observed from the examination of the Ru–Ru bond distances. It is noteworthy that the interstitial carbido atom inhibits the structural rearrangement of the octahedron into the bicapped tetrahedron, as in the case of the transformation of $[\text{Os}_6(\text{CO})_{16}]^{2-}$ into $\text{Os}_6(\text{CO})_{16}$ [11], which is expected from the PSEP approach.

The direct formation of the unsaturated cluster **6**

from the reaction of **2** with dihydrogen suggests a dissociative pathway as shown in eqn. (1).



If an associative pathway was operative a saturated hydrido (**5**, see below) should be formed (eqn. (2)), which was not the case.



Treatment of **3** in methanol with dihydrogen at 130°C also afforded **6** in good yield. In this case, the μ - η^3 -allyl ligand was thermally activated to the η^1 -allyl ligand, to provide a coordination site for dihydrogen, and then elimination of propylene left **6**.

As mentioned above, hydrogenation of olefins could only be initiated at higher temperatures when **2** was employed. However, when **6** was used, the reaction proceeded without any induction period even at room temperature and the hydrogenation rates were the same as those when pretreated **2** was used as the catalyst. Thus **6**, a two electron deficient species with a hydrido ligand, is the true active species of the hydrogenation by **2**.

2.4. Temperature dependent ^1H NMR study of [PPN][$\text{Ru}_6\text{C}(\text{CO})_{15}\text{H}$] (**6**)

The proton NMR spectrum of **6** in CD_2Cl_2 at room temperature consists of a multiplet at δ 7.4–7.9 and a singlet at δ –20.01, whose peak areas are in a ratio of 30:1. Upon cooling, the peak at 7.4–7.9, owing to the [PPN] cation, remains unchanged, but that at δ –20.01, owing to the hydrido, was split into two singlets. A limiting spectrum in this region below –50°C showed the singlets at δ –19.88 and –20.71. The ratio of the peak areas between the two isomers is temperature dependent and the intensities are in the ratio of 1.8:1 at –50°C. The temperature dependence and the non-integral relationship of the area under these peaks suggests the presence of two isomeric species. The limiting spectrum in acetone- d_6 at –50°C was also obtained. The relative ratio of their peak areas was 2.1:1 again confirming the presence of two isomers. The equilibrium constants for low-field high-field isomers were obtained from the peak areas in the limiting spectrum, and the thermodynamic parameters were

calculated from a least-squares fit of $\ln K$ plotted against $1/T$; in CD_2Cl_2 $\Delta H = -1.36 \pm 0.06$ Kcal mol $^{-1}$, $\Delta S = -7.3 \pm 0.2$ e.u., and $K = 0.55$ (–50°C); in CD_3COCD_3 $\Delta H = -1.23 \pm 0.07$ Kcal mol $^{-1}$, $\Delta S = -7.0 \pm 0.3$ e.u., and $K = 0.47$ (–50°C). These values indicate that the low-field isomer has higher polarity, though we have no basis for this on the structures at present.

From the ^1H NMR measurements, two structural isomers of $[\text{Ru}_4(\text{CO})_{12}\text{H}_3]^-$ are assumed to be in solution, rapidly interchanging at room temperature [12], and the X-ray analyses of the corresponding complexes revealed the structures to be different only in the position of the hydrido ligands [13]. The presence of the two isomers of $[\text{Re}_7(\text{CO})_{21}\text{H}]^{2-}$ could also be deduced by ^1H NMR measurements, and two structural isomers were determined crystallographically, and shown to be different only in the position of the hydrido ligand [14].

The parameters obtained are comparable with those for the equilibrium for the two isomers of $[\text{Ru}_4(\text{CO})_{12}\text{H}_3]^-$ [12] and $[\text{Re}_7\text{C}(\text{CO})_{21}\text{H}]^{2-}$ [14].

The observed spectra indicate coalescence of the two peaks to one line; this can be achieved by rapid interchange of the isomers. The thermodynamic parameters for these merging resonances have been calculated. First, the values for the rate constant were calculated, based on the differences of chemical shift of the two peaks, then the activation energy for the coalescence could be calculated from the least-squares fit of $\ln(k/T)$ against $1/T$; in CD_2Cl_2 $\Delta H = 11.2 \pm 1.4$ Kcal mol $^{-1}$ and $\Delta S = -3.3 \pm 0.4$ e.u.. Similar values were reported for the isomers of $[\text{Ru}_4(\text{CO})_{12}\text{H}_3]^-$ [12] and $[\text{Re}_7\text{C}(\text{CO})_{21}\text{H}_2]^-$ [15].

2.5. Reaction of [PPN][$\text{Ru}_6\text{C}(\text{CO})_{15}\text{H}$] (**6**) with carbon monoxide

In order to confirm the unsaturation **6** was allowed to react under atmospheric pressure of carbon monoxide at room temperature for 30 min. Work-up of the solution afforded deep-red crystals. The IR spectrum of the product exhibited a strong band at 2009 cm^{-1} , indicating the product to be a mono-anionic hexanuclear ruthenium cluster. The ^1H NMR spectrum of the product showed a singlet at δ –18.98, attributable to a hydrido. Based on these data and elemental analysis, the complex was assumed to be a saturated mono-anionic carbido hydrido hexanuclear carbonyl cluster [PPN][$\text{Ru}_6\text{C}(\text{CO})_{16}\text{H}$] (**5**). This compound was shown to be the mono-anionic cluster that was obtained by protonation of the corresponding dianionic cluster **1** [5]. It is noteworthy that **5** does not show catalytic activity for the hydrogenation of olefins at room temperature.

2.6. Structure of [PPN][Ru₆C(CO)₁₆H] (5)

A single-crystal X-ray diffraction study of **5** has been undertaken. The cation [PPN] has been fully located but the anion [Ru₆C(CO)₁₆H]⁻ appears to be disordered. Despite the disorder, the structure of the first molecule [Ru₆C(CO)₁₆H]⁻ has been clearly established and is shown in Fig. 6. The six ruthenium atoms of the second molecule are located, but the carbonyl groups could not be fully located because of their low electron densities. The selected interatomic bond distances and angles of **5** are listed in Tables 3 and 4, respectively.

The metal frameworks of the first and the second molecules are the same as that shown in Fig. 7. The two sets of the six ruthenium atoms form octahedrons containing a common carbide atom C(0) at the center of the octahedrons. The geometry of the anionic cluster [Ru₆C(CO)₁₆H]⁻ can be regarded as a sphere in the first approximation, and hence the cluster may be apt to show spherical disorder. Neither conformational nor orientational relationships can be observed between the two molecules.

The mean Ru–Ru distances of the first and the second molecules are 2.885(9) and 2.883(19) Å, and mean Ru–carbide distances are 2.040(15) and 2.05(7) Å, respectively. These values are almost identical to those of **4** [5].

As shown in Fig. 6, there are two bridging and two semi-bridging carbonyl ligands in the first molecule.

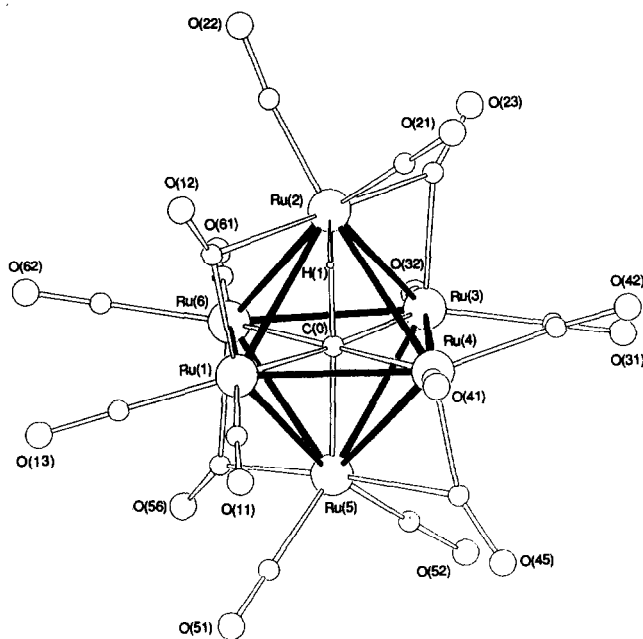


Fig. 6. The molecular structure of [Ru₆C(CO)₁₆H]⁻ (anion of **5**), showing the atom numbering scheme.

TABLE 3. Selected interatomic distances (Å) and esd values for [PPN][Ru₆C(CO)₁₆H] (**5**)

First molecule			
Ru(1)–Ru(2)	2.911(2)	Ru(6)–C(0)	2.078(13)
Ru(1)–Ru(4)	2.883(2)	Ru(1)–C(12)	2.042(13)
Ru(1)–Ru(5)	2.885(2)	Ru(1)–H(1)	2.19(9)
Ru(1)–Ru(6)	2.881(2)	Ru(2)–C(12)	2.563(14)
Ru(2)–Ru(3)	2.832(2)	Ru(2)–C(23)	2.194(13)
Ru(2)–Ru(4)	2.917(2)	Ru(2)–H(1)	1.62(9)
Ru(2)–Ru(6)	2.920(2)	Ru(3)–C(23)	2.073(11)
Ru(3)–Ru(4)	2.882(2)	Ru(4)–C(45)	1.933(15)
Ru(3)–Ru(5)	2.923(1)	Ru(4)–H(1)	2.28(10)
Ru(3)–Ru(6)	2.880(2)	Ru(5)–C(45)	2.409(21)
Ru(4)–Ru(5)	2.876(2)	Ru(5)–C(56)	2.139(17)
Ru(5)–Ru(6)	2.824(2)	Ru(6)–C(56)	2.218(11)
Ru(1)–C(0)	2.034(9)	O(12)–C(12)	1.059(17)
Ru(2)–C(0)	2.081(9)	O(23)–C(23)	1.159(14)
Ru(3)–C(0)	2.048(9)	O(45)–C(45)	1.197(20)
Ru(4)–C(0)	1.991(13)	O(56)–C(56)	1.104(16)
Ru(5)–C(0)	2.009(8)		
Second molecule			
Ru(01)–Ru(02)	2.791(5)	Ru(02)–Ru(06)	2.896(6)
Ru(01)–Ru(04)	2.952(6)	Ru(03)–Ru(04)	2.808(6)
Ru(01)–Ru(05)	2.804(8)	Ru(03)–Ru(05)	2.924(6)
Ru(01)–Ru(06)	2.852(6)	Ru(03)–Ru(06)	2.951(7)
Ru(02)–Ru(03)	2.998(10)	Ru(04)–Ru(05)	2.898(6)
Ru(02)–Ru(04)	2.893(6)	Ru(05)–Ru(06)	2.834(6)
C(0)–Ru(01)	2.093(11)	Ru(02)–C(62)	2.80(2)
C(0)–Ru(02)	1.785(12)	Ru(02)–C(012)	2.03(7)
C(0)–Ru(03)	2.033(13)	Ru(02)–C(02)	1.87(4)
C(0)–Ru(04)	2.018(10)	Ru(06)–C(06)	1.93(8)
C(0)–Ru(05)	2.278(11)	O(13)–C(01)	1.12(5)
C(0)–Ru(06)	2.105(10)	C(62)–C(012)	0.95(8)
Ru(01)–C(62)	2.75(2)	O(02)–C(02)	1.07(5)
Ru(01)–C(01)	1.89(6)	O(06)–C(06)	1.20(9)
Ru(01)–C(012)	2.01(6)		

The bridging ligands span two mutually-perpendicular pairs of edges (*i.e.*, Ru(1)–Ru(2)–Ru(3) and Ru(4)–Ru(5)–Ru(6)). The mean Ru–Ru bond lengths of non-bridged edges range from 2.881(2) to 2.923(1) Å, and those of bridged edges from 2.824(2) to 2.832(2) Å. Thus, bridging seems to induce a significant contraction of the Ru–Ru bonds, as shown in the case of **6**. Each ruthenium atom carries two terminal carbonyl ligands, and the twelve terminal carbonyl groups seem to be essentially normal with mean dimensions Ru–C 1.87(1), C–O 1.15(1) Å, and Ru–C–O angles higher than 172(1)° (Ru(1)–C(11)–O(11)). So far as metal, carbide, and carbonyl distributions are discussed, the overall arrangement of the first molecule is isostructural with that of the cluster dianion [Ru₆C(CO)₁₆]²⁻ of [AsPh₄]₂[Ru₆C(CO)₁₆] [9] of approximate overall *D*_{2d} symmetry.

A hydrido atom detected by ¹H NMR at δ –18.98 was located by the differential-Fourier syntheses as a terminal ligand with a Ru(2)–H(1) distance 1.62(9) Å, shorter than that of the bridging ligand in **4** or **6**. The

hydrido is 1.08(10) Å above the triangle plane of Ru(1)–Ru(2)–Ru(4), with slight interactions with Ru(1) (2.19(9) Å) and Ru(4) (2.28(10) Å). In terms of overall electron counting, the cluster anion of **5** contains 86 valence electrons, as predicted for an octahedron by PSEP approach [10]. Consequently, **5** is an electronically-saturated cluster.

We have reported the structure of **4**. Temperature varying ¹H NMR measurements did not show the presence of the isomeric forms of the anion of **4** or **5** in solution. The cluster anion of **4** is identical with that of **5** in solution, but different in the crystal. Comparison

TABLE 4. Selected interatomic angles (°) and esd values for [PPN][Ru₆C(CO)₁₆H] (**5**)

First molecule			
Ru(2)–Ru(1)–H(1)	33(2)	C(21)–Ru(2)–H(1)	64(4)
Ru(4)–Ru(1)–H(1)	51(3)	C(22)–Ru(2)–C(23)	92.2(7)
C(0)–Ru(1)–C(11)	134.7(7)	C(22)–Ru(2)–H(1)	122(3)
C(0)–Ru(1)–C(12)	104.9(4)	C(23)–Ru(2)–H(1)	135(4)
C(0)–Ru(1)–C(13)	129.0(6)	C(0)–Ru(3)–C(23)	97.4(4)
C(0)–Ru(1)–H(1)	66(2)	C(0)–Ru(3)–C(31)	133.6(5)
C(11)–Ru(1)–C(12)	92.0(6)	C(0)–Ru(3)–C(32)	132.6(6)
C(11)–Ru(1)–C(13)	88.3(8)	C(23)–Ru(3)–C(31)	94.7(5)
C(11)–Ru(1)–H(1)	98(3)	C(23)–Ru(3)–C(32)	99.1(5)
C(12)–Ru(1)–C(13)	97.6(7)	C(31)–Ru(3)–C(32)	88.7(6)
C(12)–Ru(1)–H(1)	50(3)	Ru(1)–Ru(4)–H(1)	49(3)
C(13)–Ru(1)–H(1)	146(3)	Ru(2)–Ru(4)–H(1)	34(2)
Ru(1)–Ru(2)–H(1)	48(3)	C(0)–Ru(4)–C(41)	131.1(7)
Ru(4)–Ru(2)–H(1)	51(3)	C(0)–Ru(4)–C(42)	131.3(5)
C(0)–Ru(2)–C(12)	87.5(4)	C(0)–Ru(4)–C(45)	100.3(7)
C(0)–Ru(2)–C(21)	122.0(6)	C(0)–Ru(4)–H(1)	65(3)
C(0)–Ru(2)–C(22)	146.2(8)	C(41)–Ru(4)–C(42)	88.9(7)
C(0)–Ru(2)–C(23)	92.8(4)	C(41)–Ru(4)–C(45)	99.2(7)
C(0)–Ru(2)–H(1)	75(3)	C(41)–Ru(4)–H(1)	76(3)
C(12)–Ru(2)–C(21)	89.7(6)	C(42)–Ru(4)–C(45)	98.5(7)
C(12)–Ru(2)–C(22)	88.4(7)	C(42)–Ru(4)–H(1)	112(3)
C(12)–Ru(2)–C(23)	178.3(6)	C(45)–Ru(4)–H(1)	148(2)
C(12)–Ru(2)–H(1)	44(4)	C(0)–Ru(5)–C(45)	85.4(5)
C(21)–Ru(2)–C(22)	91.6(9)	C(0)–Ru(5)–C(51)	122.0(6)
C(21)–Ru(2)–C(23)	88.8(6)	C(0)–Ru(5)–C(52)	125.1(7)
C(0)–Ru(5)–C(56)	98.0(5)	Ru(1)–C(12)–O(12)	156.3(12)
C(45)–Ru(5)–C(51)	87.6(7)	Ru(2)–C(12)–O(12)	126.2(10)
C(45)–Ru(5)–C(52)	84.5(9)	Ru(2)–C(23)–Ru(3)	83.1(4)
C(45)–Ru(5)–C(56)	176.5(5)	Ru(2)–C(23)–O(23)	134.4(10)
C(51)–Ru(5)–C(52)	111.3(8)	Ru(3)–C(23)–O(23)	142.5(10)
C(51)–Ru(5)–C(56)	90.1(7)	Ru(4)–C(45)–Ru(5)	82.2(7)
C(52)–Ru(5)–C(56)	93.8(9)	Ru(4)–C(45)–O(45)	154.2(17)
C(0)–Ru(6)–C(56)	93.6(5)	Ru(5)–C(45)–O(45)	123.3(13)
C(0)–Ru(6)–C(61)	135.7(6)	Ru(5)–C(56)–Ru(6)	80.8(5)
C(0)–Ru(6)–C(62)	139.2(5)	Ru(5)–C(56)–O(56)	140.2(11)
C(56)–Ru(6)–C(61)	94.3(5)	Ru(6)–C(56)–O(56)	138.4(12)
C(56)–Ru(6)–C(62)	94.4(5)	Ru(1)–H(1)–Ru(2)	98(5)
C(61)–Ru(6)–C(62)	83.4(6)	Ru(1)–H(1)–Ru(4)	80(3)
Ru(1)–C(12)–Ru(2)	77.5(4)	Ru(2)–H(1)–Ru(4)	95(4)
Second molecule			
Ru(01)–C(01)–O(13)	154(4)	Ru(02)–C(012)–C(62)	136(4)
Ru(01)–C(012)–C(62)	133(4)	Ru(02)–C(02)–O(02)	163(4)
Ru(01)–C(012)–Ru(01)	87(3)	Ru(06)–C(06)–O(06)	160(6)

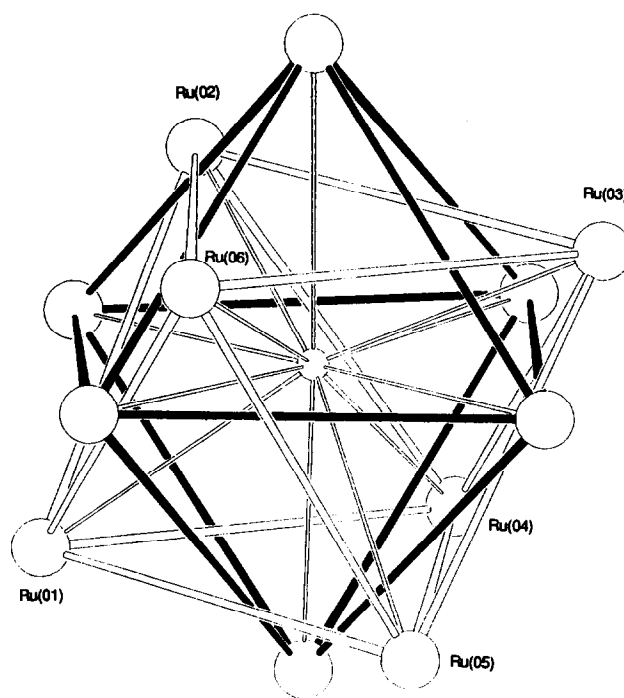


Fig. 7. The two components of the disordered cluster [Ru₆C(CO)₁₆H]⁻ (anion of **5**), viewed from the same direction as in Fig. 6. Carbonyl and hydrido ligands are omitted for clarity.

of these cluster anions shows that the major differences are the overall arrangement of the carbonyl and hydrido ligands, because the anion of **4** has three bridging carbonyl and a bridging hydrido ligands.

Similar conformational isomers are reported for the dianions of [Et₄N]₂[Ru₆C(CO)₁₆] [16] and [AsPh₄]₂[Ru₆C(CO)₁₆]. Though distinct isomers of the cluster anion [Ru₆C(CO)₁₆]²⁻ have not been confirmed in solution, two structural isomers of different carbonyl distribution have been obtained in the solid state bearing different counter cations. Structures of [Ru₆C(CO)₁₆H]⁻ therefore are another example of the two isomeric forms of a high-nuclearity metal carbonyl cluster anion, different only in their ligand distribution, to be characterized by X-ray analyses.

3. Experimental details

3.1. General

Clusters [PPN]₂[Ru₆C(CO)₁₆] (**1**) [3], [PPN][Ru₆C(CO)₁₆(CH₃)] (**2**) [4], and [PPN][Ru₆C(CO)₁₅(C₃H₅)] (**3**) [4] were prepared according the literature. Ruthenium metal catalyst (0.5% ruthenium on activated carbon) was purchased from Nippon Engelhard Industries. All the chemicals used for hydrogenations – methyl butenes (**3m1b**, **2m2b**, and **2m1b**), cyclohexanone, benzene, isoprene, nitrobenzene, and THF – were distilled prior to use. Other chemicals were used

as received, unless otherwise stated. All reactions and manipulations were carried out under argon. IR and NMR spectra were recorded on a Jasco A-202 spectrophotometer and a Jeol GSX-500 spectrometer, respectively.

3.2. Hydrogenation

Typically, a 50-ml stainless steel pressure bottle, containing a teflon-coated stirring bar and $[PPN][Ru_6C(CO)_{16}(CH_3)]$ (**2**) (2.50 mg, 1.54×10^{-3} mmol), was charged with THF (15 ml) against a stream of argon, then pressurized to 100 atm with dihydrogen and immersed in a water bath at 80°C. The mixture was stirred magnetically. After 2 h the vessel was transferred into an iced water bath for 30 s and then into a dry ice-methanol bath for 3 min, with stirring. After the gas was released, 3-methyl-1-butene (**3m1b**) (0.559 ml, 5.00 mmol) was introduced against a stream of argon, and the vessel pressurized again with dihydrogen to 100 atm. Hydrogenation started immediately after immersion of the vessel in the water bath at 60°C. After every 30 min the reaction vessel was cooled in the same manner as described above, and a sample of the solution was taken by a syringe. The reaction was then restarted by admitting dihydrogen. The hydrogenation samples were analyzed by GLC on a column of 25wt% sebaconitrile on Uniport C (olefins), 10wt% benton 34 on Neopak 1A (cyclohexanone), and 5wt% bis(2,3-dihydroxypropyl) ether on Chromosorb (nitrobenzene).

The conversion was proportional to the reaction time without an induction period, and reached *ca* 6% after 3 h. The reaction rate was proportional to the amount of **2** and independent of the concentration of the substrate. Thus, the data could be analyzed, and was based on the zero-order of the reaction with respect to the substrate. Isomerization was neglected for the determination of the hydrogenation rate, because the concentration of the substrate remained almost constant while the conversion remained low.

When Ru-charcoal was used as the catalyst, catalyst pre-treatment and hydrogenation reactions were conducted in the same manner described above. No induction periods were observed.

The turn-over frequencies of **3m1b** hydrogenation by **2** and Ru-charcoal were 0.087/s and 2.68/s, respectively, assuming that all the metal atoms of Ru-charcoal were active sites.

3.3. Reaction of $[PPN][Ru_6C(CO)_{16}(CH_3)]$ (**2**) and $[PPN][Ru_6C(CO)_{15}(C_3H_5)]$ (**3**) with dihydrogen

Cluster **3** (10.00 mg, 6.17×10^{-3} mmol) and methanol (2 ml) were placed in a Pyrex glass ampoule (*ca.* 100 ml) with fine drawn neck. The ampoule was

then charged with 1 atm of dihydrogen and sealed quickly with a frame. Immediate cooling of the hot spot by blowing a quick stream of air is essential, because the vapor of methanol will otherwise decompose on the hot glass wall in the presence of dihydrogen to yield methane in significant amounts. The ampoule was set in a stainless steel pressure vessel and the vessel was then placed in an oven at 130°C. After 1 h the ampoule was opened in degassed water. The total amount of the gas, collected above the water, was measured, and the composition of the gas analyzed by GLC on a column of alumina and 25 wt% sebaconitrile on Uniport C. In the gas phase, propylene and propane were produced in 94% yield, based on **3**, and no other hydrocarbons were detected. The blank test showed formation of methane of not more than 0.5% equivalent of **3** and of no other hydrocarbons.

The reaction of **2** was carried out similarly. Analyses of the reaction products showed the formation of methane, but of no other hydrocarbons.

3.4. Preparation of $[PPN][Ru_6C(CO)_{15}H]$ (**6**)

Cluster **2** (105 mg, 0.065 mmol) and methanol (20 ml) were added to a 100 ml autoclave, equipped with an inner glass tube and a teflon-coated stirring bar. The autoclave was pressurized to 100 atm with dihydrogen and heated to 100°C with stirring, and kept at 100°C for 1 h. After cooling to room temperature, the solution was filtered and concentrated to *ca.* 2 ml at 50°C. Then the solution was allowed to stand overnight at room temperature. Red crystals had formed, and were collected, washed with an ethanol-hexane (1:1) mixture and dried *in vacuo* (80 mg, 0.051 mmol, 78% yield). IR (CH_2Cl_2): $\nu(C=O)$ 2070w, 2009s, 1952w, and 1814m cm^{-1} . 1H NMR (acetone- d_6): δ 7.4–7.9 (30H, m, phenyl), –20.03 (1H, s, hydrido); (CD_2Cl_2): δ 7.4–7.9 (30H, m, phenyl), –20.01 (1H, s, hydrido). Anal. Found: C, 39.28, H, 1.98; N, 0.93. $C_{52}H_{31}NO_{15}P_2Ru_6$ calcd.: C, 39.58; H, 1.98; N, 0.89%.

The analogous reaction of **3** (90 mg, 0.056 mmol) with dihydrogen at 130°C also gave **6** (62 mg, 0.039 mmol, 71% yield).

3.5. Preparation of $[PPN][Ru_6C(CO)_{16}H]$ (**5**)

A solution of **6** (50 mg, 0.032 mmol) in CH_2Cl_2 (10 ml) was placed in a 100-ml reaction vessel and then carbon monoxide was introduced (1 atm). After stirring for 30 min at room temperature the solution was filtered and concentrated (1 ml). Methanol (1 ml) was added and the mixture was then kept at 0°C for 1 h. Red crystals were collected, washed with ethanol-hexane and dried *in vacuo* (38 mg, 0.024 mmol, 75% yield). IR (CH_2Cl_2): $\nu(C=O)$ 2065w, 2009vs, 1959w, 1864w(br), 1815m(br) cm^{-1} . 1H NMR (acetone- d_6): δ

7.5–7.8 (30H, m, phenyl), –18.98 (1H, s, hydrido). The spectrum did not change, not even if the temperature was lowered as far as –70°C. Anal. Found: C, 39.40; H, 2.00; N, 0.85. $C_{53}H_{31}NO_{16}P_2Ru_6$ calcd.: C, 39.63; H, 1.95; N, 0.87%.

Cluster 5 could also be obtained by the protonation of $[PPN]_2[Ru_6C(CO)_{16}]$ (1), as described in the preceding paper [5].

3.6. Structure determination

3.6.1. Data collection

Red single crystals of 6 suitable for X-ray measurements were obtained by recrystallization from hot methanol. The crystal was fixed with the mother liquor in a glass capillary filled with argon. Deep-red single crystals of 5 were obtained by diffusion of dry hexane into a dry CH_2Cl_2 solution in a tube (8 mm i.d.) at room temperature for a few days. The crystal was fixed with Apiezon grease L in a glass capillary filled with argon.

Unit cell dimensions were derived from the least-squares fit of the angular settings of 20 reflections with $20^\circ < 2\theta < 25^\circ$. Intensity data were collected at 21°C by use of Rigaku AFC-4 (for 6) and Enraf-Nonius CAD4

(for 4) fourcircle automated diffractometers with graphite-monochromatized Mo-K α radiation. Crystal data and experimental details are listed in Table 5.

3.6.2. Structure analysis and refinement for 6

The survey of the data set revealed no systematic extinctions and no symmetry other than the Friedel condition ($\bar{1}$). Thus, the crystal belongs to the triclinic class with space group $P1$ or $P\bar{1}$. The latter centrosymmetric possibility was strongly indicated by the cell volume (consistent with $Z = 2$) and was confirmed by the successful refinement of the structure for this higher-symmetry space group. Data were not corrected for absorption because deviations of F_o for axial reflections at $\chi \approx 90$ were within $\pm 5\%$. Throughout the analysis, the analytical form of the scattering factor [17a] for the appropriate neutral atom used in calculating F_c was corrected for both real ($\Delta f'$) and imaginary ($\Delta f''$) components of anomalous dispersions [17b]. The structure was solved by direct methods by use of the program MULTAN [18], which located six ruthenium atoms of the asymmetric unit. The remaining non-hydrogen atoms and 29 hydrogen atoms were located from subsequent difference Fourier syntheses. The remaining two phenyl hydrogens were not located. They

TABLE 5. Crystallographic data

	[PPN][Ru ₆ C(CO) ₁₆ H] (5)	[PPN][Ru ₆ C(CO) ₁₅ H] (6)
Formula	C ₅₃ H ₃₁ NO ₁₆ P ₂ Ru ₆	C ₅₂ H ₃₁ NO ₁₅ P ₂ Ru ₆
Formula weight	1606.19	1578.18
Crystal system	Triclinic	Triclinic
Space group (No.)	$P\bar{1}$ (2)	$P\bar{1}$ (2)
<i>a</i> , Å	14.401(2)	18.703(4)
<i>b</i> , Å	17.522(3)	15.924(4)
<i>c</i> , Å	12.535(2)	9.518(2)
α , °	109.269(14)	102.60(2)
β , °	97.055(13)	91.58(2)
γ , °	72.634(12)	94.01(2)
Cell volume, Å ³	2849	2757
<i>Z</i>	2	2
<i>D</i> _{calcd} , g cm ⁻³	1.873	1.904
Temperature, °C	21	21
Size (mm)	0.18 × 0.29 × 0.63	0.17 × 0.46 × 0.50
λ (Mo-K α), Å	0.71073	0.71073
2 θ limit, °	55	55
Unique obsd. reflections	7928 ($F \geq 3\sigma$)	8513 ($F \geq 3\sigma$)
No. of parameters	786	802
Linear abs. coeff. μ , cm ⁻¹	16.42	16.96
<i>F</i> (000), e	1556	1528
Correction made	ψ scan	no
Transmission coeff.	0.9174–0.9997	
<i>R</i>	0.0666	0.0506
<i>R</i> _w , (<i>w</i>)	0.0635 (<i>w</i> = 1)	0.0468 (<i>w</i> = 1/ σ)
Goodness of fit indicator	2.76	2.87
$\delta\rho_{map}$, e Å ⁻³	1.60	1.26

TABLE 6. Atomic coordinates and equivalent temperature factors (\AA^2) for $[\text{PPN}][\text{Ru}_6\text{C}(\text{CO})_{15}\text{H}]$ (6) with esd values in parentheses

Atom	x	y	z	B_{eq}^a
Ru(1)	0.20752(3)	0.16063(4)	0.49504(6)	3.5
Ru(2)	0.17089(3)	0.31148(4)	0.70653(6)	3.4
Ru(3)	0.28733(3)	0.41248(4)	0.62017(7)	3.8
Ru(4)	0.18459(3)	0.31752(4)	0.40017(6)	3.5
Ru(5)	0.32691(3)	0.26117(4)	0.40481(7)	3.9
Ru(6)	0.31579(3)	0.25342(4)	0.70201(6)	3.5
P(1)	0.17045(9)	-0.18236(12)	1.05543(20)	3.4
P(2)	0.33158(9)	-0.20514(12)	1.05235(20)	3.4
O(11)	0.23408(42)	-0.00942(43)	0.56999(94)	8.7
O(12)	0.08711(34)	0.06067(40)	0.29706(74)	6.7
O(21)	0.02873(29)	0.36645(40)	0.61317(72)	6.3
O(22)	0.10364(39)	0.31283(62)	0.99197(75)	9.2
O(23)	0.19933(32)	0.50109(39)	0.86084(69)	6.5
O(31)	0.27122(39)	0.57242(43)	0.50614(88)	8.1
O(32)	0.41683(32)	0.50874(40)	0.79444(80)	7.1
O(41)	0.13300(40)	0.48333(43)	0.33763(88)	8.3
O(42)	0.05209(33)	0.22588(43)	0.22578(76)	7.0
O(45)	0.26119(33)	0.30460(52)	0.12262(64)	7.2
O(51)	0.40357(42)	0.16309(59)	0.15146(74)	9.6
O(52)	0.43532(33)	0.40990(45)	0.39944(84)	7.3
O(56)	0.45842(26)	0.20453(40)	0.56807(60)	5.4
O(61)	0.40623(35)	0.35411(44)	0.96327(67)	6.9
O(62)	0.33107(36)	0.09214(46)	0.81737(82)	7.6
N	0.25222(30)	-0.18801(45)	1.08683(71)	4.8
C(0)	0.24766(36)	0.28631(46)	0.55349(71)	3.1
C(11)	0.22305(44)	0.05630(54)	0.54494(103)	5.4
C(12)	0.13359(41)	0.10024(50)	0.36852(87)	4.6
C(21)	0.08450(44)	0.34621(54)	0.63785(95)	5.2
C(22)	0.12874(42)	0.31130(63)	0.88392(91)	5.5
C(23)	0.21386(37)	0.44136(51)	0.77389(84)	4.4
C(31)	0.27620(45)	0.51178(56)	0.54688(102)	5.5
C(32)	0.36722(41)	0.47148(47)	0.73103(92)	4.7
C(41)	0.15410(46)	0.42231(58)	0.36142(97)	5.6
C(42)	0.10208(41)	0.25833(51)	0.29159(88)	4.6
C(45)	0.25138(43)	0.30181(59)	0.23964(89)	5.1
C(51)	0.37571(47)	0.19667(65)	0.24671(88)	5.8
C(52)	0.39019(43)	0.35862(59)	0.40987(101)	5.4
C(56)	0.40052(38)	0.22670(47)	0.57783(79)	4.1
C(61)	0.37384(41)	0.31953(55)	0.86317(85)	4.8
C(62)	0.32354(40)	0.15094(59)	0.77185(91)	5.0
C(A1)	0.15453(34)	-0.08674(44)	0.99136(70)	3.4
C(A2)	0.20068(39)	-0.01305(49)	1.04133(85)	4.3
C(A3)	0.18852(50)	0.06366(53)	0.99952(100)	5.6
C(A4)	0.13078(58)	0.06508(59)	0.90849(110)	6.6
C(A5)	0.08480(57)	-0.00493(62)	0.86172(119)	7.1
C(A6)	0.09578(45)	-0.08151(56)	0.90345(97)	5.5
C(B1)	0.12768(37)	-0.27385(45)	0.92645(85)	4.1
C(B2)	0.14819(51)	-0.28863(60)	0.78549(92)	5.9
C(B3)	0.11401(59)	-0.35720(65)	0.68263(103)	7.2
C(B4)	0.06231(56)	-0.40891(60)	0.72191(130)	7.9
C(B5)	0.04261(53)	-0.39761(61)	0.86018(138)	7.7
C(B6)	0.07515(44)	-0.32795(54)	0.96625(106)	5.7
C(C1)	0.12655(37)	-0.17463(48)	1.22196(80)	4.0
C(C2)	0.05694(47)	-0.14599(62)	1.23433(101)	5.9
C(C3)	0.02347(59)	-0.13850(69)	1.36284(121)	7.6
C(C4)	0.05728(67)	-0.15861(86)	1.47532(121)	9.0
C(C5)	0.12499(72)	-0.18780(100)	1.46632(123)	10.0
C(C6)	0.16082(55)	-0.19650(81)	1.33655(103)	7.5
C(D1)	0.38970(35)	-0.11639(44)	1.15366(74)	3.6
C(D2)	0.45646(40)	-0.09432(53)	1.10650(89)	4.7
C(D3)	0.49973(43)	-0.02654(60)	1.19001(109)	5.9

TABLE 6 (continued)

Atom	x	y	z	B_{eq}^a
C(D4)	0.47679(49)	0.01934(56)	1.31988(101)	5.7
C(D5)	0.41049(49)	-0.00417(58)	1.36745(94)	5.6
C(D6)	0.36732(40)	-0.07088(50)	1.28431(84)	4.4
C(E1)	0.35188(35)	-0.21449(45)	0.86602(75)	3.6
C(E2)	0.39132(46)	-0.28050(51)	0.79251(87)	4.9
C(E3)	0.40565(50)	-0.28494(60)	0.65189(96)	5.8
C(E4)	0.38024(46)	-0.22734(62)	0.57767(85)	5.5
C(E5)	0.34157(46)	-0.16016(61)	0.65039(96)	5.6
C(E6)	0.32721(43)	-0.15538(55)	0.79429(89)	4.9
C(F1)	0.35397(38)	-0.30042(47)	1.10792(75)	3.8
C(F2)	0.42027(43)	-0.30840(58)	1.17054(102)	5.5
C(F3)	0.43614(56)	-0.38347(68)	1.21004(115)	7.0
C(F4)	0.38494(62)	-0.45098(63)	1.19191(107)	7.0
C(F5)	0.31753(64)	-0.44422(65)	1.13107(124)	7.7
C(F6)	0.30287(50)	-0.36974(57)	1.08916(106)	6.0
H(1)	0.1446(42)	0.1835(51)	0.6342(85)	6.6(21)
H(A2)	0.2398(34)	-0.0207(41)	1.0982(69)	3.9(15)
H(A3)	0.2254(46)	0.1158(55)	1.0381(92)	7.4(24)
H(A4)	0.1203(45)	0.1224(54)	0.8828(89)	7.3(22)
H(A5)	0.0416(62)	-0.0085(74)	0.7932(125)	12.5(37)
H(A6)	0.0665(44)	-0.1310(53)	0.8489(90)	7.0(22)
H(B2)	0.1788(42)	-0.2447(51)	0.7491(86)	6.5(21)
H(B3)	0.1319(48)	-0.3669(58)	0.5779(96)	8.2(25)
H(B4)	0.0389(60)	-0.4563(71)	0.6547(121)	11.9(35)
H(B5)	0.0155(50)	-0.4452(60)	0.8982(100)	8.8(26)
H(B6)	0.0615(50)	-0.3178(60)	1.0775(100)	8.7(26)
H(C2)	0.0324(67)	-0.1375(80)	1.1258(136)	13.9(40)
H(C3)	-0.0365(70)	-0.1173(83)	1.3706(141)	14.6(43)
H(C4)	0.0310(60)	-0.1627(72)	1.5684(121)	12.0(35)
H(C5)	0.1465(74)	-0.2092(89)	1.5419(148)	15.5(46)
H(D2)	0.4739(42)	-0.1193(51)	1.0095(86)	6.5(21)
H(D3)	0.5428(40)	-0.0139(47)	1.1532(79)	5.6(19)
H(D4)	0.5056(40)	0.0654(49)	1.3808(82)	5.8(19)
H(D5)	0.3973(60)	0.0349(72)	1.4744(120)	11.8(34)
H(D6)	0.3231(32)	-0.0848(39)	1.3235(65)	3.4(14)
H(E2)	0.4030(36)	-0.3267(43)	0.8486(72)	4.4(16)
H(E3)	0.4258(52)	-0.3322(63)	0.5902(104)	9.4(28)
H(E4)	0.3951(50)	-0.2344(59)	0.4734(100)	8.7(26)
H(E5)	0.3322(45)	-0.1130(54)	0.6045(90)	7.4(22)
H(E6)	0.3059(52)	-0.1063(62)	0.8436(105)	9.3(28)
H(F2)	0.4541(35)	-0.2681(42)	1.1777(70)	4.1(15)
H(F4)	0.3925(57)	-0.5105(68)	1.2310(114)	10.7(32)
H(F5)	0.2802(43)	-0.4891(52)	1.1278(86)	6.5(21)
H(F6)	0.2629(70)	-0.3650(83)	1.0443(141)	14.4(43)

^a $B_{\text{eq}} = \frac{1}{3}(\Sigma_i \Sigma_j B_{ij} a_i a_j)$ for non-hydrogen atoms. Hydrogen atoms were refined isotropically.

were refined by the block-diagonal least-squares method [19], with anisotropic thermal parameters for non-hydrogen atoms and isotropic thermal parameter for hydrogen atoms. The final $R(F)$ and $R_w(F)$ values are 5.06% and 4.68% with the weighting scheme $w = 1/\sigma$. The final difference Fourier synthesis showed no unexpected features, with the highest peak 1.0 e \AA^{-3} within the covalent radius of the ruthenium atom. Final positional and thermal parameters are listed in Table 6.

TABLE 7. Atomic coordinates and equivalent temperature factors (\AA^2) for [PPN][Ru₆C(CO)₁₆H] (5) with esd values in parentheses

Atom	x	y	z	B_{eq}^a
<i>First molecule</i>				
Ru(1)	0.62539(8)	0.21394(8)	0.40720(8)	5.7
Ru(2)	0.53871(8)	0.33779(8)	0.61444(11)	6.1
Ru(3)	0.70014(7)	0.27274(7)	0.74315(8)	4.6
Ru(4)	0.59853(8)	0.15879(7)	0.59114(8)	5.3
Ru(5)	0.79125(8)	0.14840(7)	0.53720(10)	5.6
Ru(6)	0.73576(8)	0.32116(7)	0.55693(9)	5.1
P(1)	0.04663(17)	0.32398(15)	0.18482(19)	4.0
P(2)	0.21721(17)	0.24663(15)	0.03787(19)	4.1
O(11)	0.56904(95)	0.07042(87)	0.23904(107)	11.9
O(12)	0.42922(74)	0.32883(79)	0.36507(84)	9.5
O(13)	0.71892(74)	0.23541(72)	0.21652(79)	10.8
O(21)	0.35034(69)	0.31512(72)	0.66498(101)	9.2
O(22)	0.43498(122)	0.52053(89)	0.64000(129)	14.5
O(23)	0.53570(73)	0.41815(58)	0.87645(78)	7.3
O(31)	0.70731(67)	0.20017(61)	0.92650(79)	6.9
O(32)	0.85006(76)	0.35439(72)	0.88099(85)	8.6
O(41)	0.44999(107)	0.07949(98)	0.44792(110)	14.0
O(42)	0.51293(72)	1.14649(70)	0.79076(80)	7.8
O(45)	0.74616(88)	-0.01139(64)	0.57187(97)	9.4
O(51)	0.83726(77)	0.02255(63)	0.29873(86)	8.6
O(52)	0.93571(96)	0.08870(90)	0.71210(120)	12.4
O(56)	0.94831(57)	0.21592(54)	0.48467(67)	5.6
O(61)	0.83707(84)	0.44515(67)	0.71396(92)	8.9
O(62)	0.74020(95)	0.40543(80)	0.38315(101)	10.6
N	0.12930(54)	0.31602(45)	0.10724(63)	4.6
C(0)	0.66478(68)	0.23868(64)	0.57395(78)	4.8
C(11)	0.58499(109)	0.12998(102)	0.30271(123)	7.8
C(12)	0.49347(95)	0.29893(101)	0.40286(117)	6.8
C(13)	0.68110(106)	0.22749(106)	0.29339(115)	7.3
C(21)	0.42245(101)	0.32250(95)	0.64356(129)	6.9
C(22)	0.47835(156)	0.45037(105)	0.62562(161)	10.8
C(23)	0.57455(93)	0.36911(78)	0.79622(106)	5.5
C(31)	0.70146(81)	0.22513(78)	0.85956(111)	5.2
C(32)	0.79257(103)	0.32637(94)	0.82857(109)	6.5
C(41)	0.50789(131)	0.11262(118)	0.50273(131)	9.2
C(42)	0.54415(91)	0.15436(83)	0.72009(102)	5.4
C(45)	0.70675(127)	0.05876(102)	0.56988(130)	8.2
C(51)	0.81758(129)	0.06826(96)	0.38524(137)	8.3
C(52)	0.87998(142)	0.11440(133)	0.64147(208)	12.7
C(56)	0.87358(90)	0.22137(82)	0.50459(101)	5.3
C(61)	0.79713(100)	0.39876(81)	0.65515(115)	6.2
C(62)	0.74296(98)	0.37671(84)	0.45136(113)	9.1
C(A1)	0.07984(68)	0.36094(55)	0.33209(75)	4.4
C(A2)	0.01743(73)	0.37442(62)	0.41574(83)	5.3
C(A3)	0.04518(90)	0.40049(71)	0.52884(90)	6.7
C(A4)	0.13390(85)	0.41415(74)	0.55685(88)	6.8
C(A5)	0.19610(83)	0.40436(74)	0.47624(96)	6.9
C(A6)	0.16845(74)	0.37668(63)	0.36296(81)	5.3
C(B1)	0.01253(64)	0.22942(54)	0.16332(73)	4.2
C(B2)	0.04138(76)	0.18276(60)	0.23817(81)	5.3
C(B3)	0.01603(90)	0.10838(70)	0.21657(99)	6.7
C(B4)	-0.03768(85)	0.08258(68)	0.12118(102)	6.8
C(B5)	-0.06527(90)	0.12488(74)	0.04670(102)	7.1
C(B6)	-0.04007(75)	0.19791(64)	0.06464(87)	5.5
C(C1)	-0.06116(69)	0.40125(57)	0.15764(71)	4.6
C(C2)	-0.04803(84)	0.46722(65)	0.12925(89)	6.1
C(C3)	-0.13173(96)	0.52926(72)	0.11144(99)	7.2
C(C4)	-0.021974(89)	0.52306(75)	0.12277(98)	7.5
C(C5)	-0.23350(84)	0.45870(78)	0.15167(104)	7.4

TABLE 7 (continued)

Atom	x	y	z	B_{eq}^a
C(C6)	-0.15380(77)	0.39928(69)	0.17032(91)	6.0
C(D1)	0.25074(63)	0.14740(59)	0.06699(77)	4.5
C(D2)	0.23226(79)	0.07698(69)	-0.01097(95)	6.2
C(D3)	0.25782(102)	0.00271(78)	0.01762(122)	8.8
C(D4)	0.29417(112)	0.00220(87)	0.12012(137)	9.7
C(D5)	0.31240(101)	0.07186(87)	0.19884(117)	8.7
C(D6)	0.28974(83)	0.14621(72)	0.17225(98)	6.5
C(E1)	0.32252(69)	0.28566(64)	0.06803(74)	4.9
C(E2)	0.41438(79)	0.23123(78)	0.05253(88)	6.7
C(E3)	0.49928(98)	0.25699(98)	0.06717(114)	9.2
C(E4)	0.48196(98)	0.33925(102)	0.09561(110)	9.4
C(E5)	0.39456(114)	0.40124(88)	0.11496(115)	9.3
C(E6)	0.31014(85)	0.37007(77)	0.09944(94)	6.8
C(F1)	0.18947(69)	0.22778(63)	-0.11142(73)	4.9
C(F2)	0.26397(91)	0.18244(94)	-0.18845(95)	8.2
C(F3)	0.24011(98)	0.17509(98)	-0.30259(102)	9.2
C(F4)	0.15053(104)	0.20126(95)	-0.33744(99)	8.9
C(F5)	0.07855(98)	0.24403(89)	-0.26619(108)	8.8
C(F6)	0.09844(84)	0.25811(74)	-0.14853(88)	6.5
H(1)	0.5030(66)	0.2619(57)	0.5214(76)	3.8(21) ^b
<i>Second molecule</i>				
Ru(01)	0.75630(28)	0.21500(27)	0.44247(34)	4.7
Ru(02)	0.64770(33)	0.34936(27)	0.61117(43)	5.8
Ru(03)	0.57967(33)	0.22869(40)	0.68382(42)	7.0
Ru(04)	0.77941(28)	0.21121(25)	0.67808(34)	4.4
Ru(05)	0.69406(33)	0.09653(25)	0.49932(36)	5.0
Ru(06)	0.55337(30)	0.23309(31)	0.44848(36)	5.2
O(02)	0.5109(21)	0.5083(18)	0.6056(24)	4.3(6) ^b
O(06)	0.3662(31)	0.1991(27)	0.4941(36)	8.3(10) ^b
C(01)	0.7546(36)	0.2171(31)	0.2922(41)	5.1(10) ^b
C(012)	0.7351(41)	0.3402(36)	0.4895(48)	6.5(12) ^b
C(02)	0.5492(30)	0.4457(26)	0.6041(35)	4.1(8) ^b
C(06)	0.4438(48)	0.2125(42)	0.4969(56)	8.7(15) ^b

^a $B_{\text{eq}} = \frac{1}{3}(\sum_i \sum_j B_{ij} a_i a_j)$ for non-hydrogen atoms.

^b Refined isotropically.

3.6.3. Structure analysis and refinement for 5

Analogous to the manner described above, six ruthenium atoms, [PPN] cation, carbide atom, and sixteen carbonyl ligands associated with the cluster anion were located. At this stage a difference-Fourier map revealed six high peaks more than 1.0 Å apart from the ruthenium atoms. The six peaks are 2.8–4.1 Å apart from each other and about 2.0 Å from the carbide atom C(0) and constitute an octahedron. Hence the peaks were assigned as ruthenium atoms of a disordered molecule of the cluster anion [Ru₆C(CO)₁₆H]. The [PPN] component was not disordered.

Subsequent difference-Fourier syntheses located a hydrogen atom of the first cluster molecule but only four carbonyl ligands of the second molecule because of their low electron densities. Two of the oxygen atoms of the carbonyl ligands of the second molecule, the oxygen connected to C(01) and C(012), were too

close to the atoms of the first molecule, O(13) and C(62) respectively, to be refined independently, so they were treated as in the same positions.

At this stage the structure of the anion $[\text{Ru}_6\text{C}(\text{CO})_{16}\text{H}]^-$ revealed two fully located isomeric forms, the first molecule of the cluster anion with four bridging carbonyl and a terminal hydrido ligands and the anion of **4** with three bridging carbonyl and a bridging hydrido ligands [5]. However, the structure of the second molecule of **5** could not be associated with the previous two. Thus, the carbonyl ligands of the second cluster could not be fully located.

All the non-hydrogen atoms were refined with anisotropic thermal parameters, and the hydrido atom H(1) was refined with an isotropic thermal parameter. The major to minor component of the cluster anion 80.4% : 19.6% was estimated from the Fourier syntheses. The site of the carbide atom C(0) was of full occupancy, since that atom was common for the first and the second molecules. As refinement proceeded, 30 hydrogen atoms attached to the phenyl rings of the cation [PPN] were added in their idealized positions for the structure factor calculations, but their positions were not refined. The final model converged with $R(F)$ 6.66% and $R(F)_w$ 6.35% with the weighting scheme $w = 1$. The location of the carbonyl groups of the second cluster was not sufficient but the principal features of the compound are nevertheless established. Final positional and thermal parameters are listed in Table 7.

Acknowledgment

We thank Mr. K. Nakata, Mr. K. Fujiwara, and Mr. H. Taira for help in the experiments and Prof. T. Sakurai for discussion on the X-ray analyses.

References

- 1 W.L. Gladfelter and K.J. Roessellet, in D.F. Shriver, H.D. Kaesz and R.D. Adams (eds.), *The Chemistry of Metal Cluster Complexes*, VCH Publishers, New York, 1990, Chap. 7.
- 2 J.S. Bradley, *Adv. Organomet. Chem.*, **22** (1983) 1; W.L. Gladfelter, *Adv. Organomet. Chem.*, **24** (1985) 41.
- 3 C.T. Hayward and J.R. Shapley, *Inorg. Chem.*, **21** (1982) 3816.
- 4 T. Chihara, K. Aoki and H. Yamazaki, *J. Organomet. Chem.*, **383** (1990) 367.
- 5 T. Chihara and H. Yamazaki, *J. Cluster Sci.*, **3** (1992) 49.
- 6 P. Rylander, *Catalytic Hydrogenation in Organic Syntheses*, Academic Press, New York, 1979, Chap. 7.
- 7 R. Whyman, in B.F.G. Johnson (ed.), *Transition Metal Clusters*, Wiley, Chichester, 1980, p. 555.
- 8 B.F.G. Johnson, R.D. Johnson and J. Lewis, *J. Chem. Soc., A*, (1968) 2865.
- 9 B.F.G. Johnson, J. Lewis, S.W. Sankey, K. Wong, M. McPartlin and W.J.H. Nelson, *J. Organomet. Chem.*, **191** (1980) C3.
- 10 D.M.P. Mingos, *Acc. Chem. Res.*, **17** (1984) 311.
- 11 B. Tulyathan and W.E. Geiger, *J. Am. Chem. Soc.*, **107** (1985) 5960.
- 12 J.W. Koepke, J.R. Johnson, S.A.R. Knox and H.D. Kaesz, *J. Am. Chem. Soc.*, **97** (1975) 3947.
- 13 P.F. Jackson, B.F.G. Johnson, J. Lewis, M. McPartlin and W.J.H. Nelson, *J. Chem. Soc., Chem. Commun.*, (1978) 920.
- 14 T. Beringhelli, G. D'Alfonso, G. Ciani, A. Sironi and H. Molinari, *J. Chem. Soc., Dalton Trans.*, (1988) 1281.
- 15 T. Beringhelli, G. D'Alfonso, G. Ciani, A. Sironi and H. Molinari, *J. Chem. Soc., Dalton Trans.*, (1990) 1901.
- 16 G.B. Ansell and J.S. Bradley, *Acta Crystallogr.*, **B36** (1980) 1930.
- 17 (a) D.T. Cromer and J.T. Waber, in J.A. Ibers and W.C. Hamilton (eds.), *International Tables for X-Ray Crystallography*, Vol. IV, Kynoch Press, Birmingham, 1974, p. 71; (b) D.T. Cromer, in J.A. Ibers and W.C. Hamilton (eds.), *International Tables for X-Ray Crystallography*, Vol. IV, Kynoch Press, Birmingham, 1974, p. 148.
- 18 P. Main, S.E. Hull, L. Lessinger, G. Germain, J.-P. Declercq and M.M. Woolfson, *MULTAN 78*, University of York, York, England, 1978.
- 19 T. Sakurai and K. Kobayashi, *Rikagaku Kenkyusho Hokoku*, **55** (1979) 69.